NASA Technical Memorandum 102403

Mechanical Properties of Pure Nickel Alloys After Long Term Exposures to LiOH and Vacuum at 775 K

J. Daniel Whittenberger
Lewis Research Center
Cleveland, Ohio

and

E.J. Vesely, Jr.
Surface Engineering Center
IIT Research Institute
Chicago, Illinois

January 1990

NASA

(NASA-TM-102403) MECHANICAL PROPERTIES OF PURE NICKEL ALLOYS AFTER LONG TERM EXPOSURES TO LiOH AND VACUUM AT 775 K (NASA) 23 p CSCL 11F

N90-20181

Unclas
G3/26 0261708

MECHANICAL PROPERTIES OF PURE NICKEL ALLOYS AFTER LONG TERM EXPOSURES TO LiOH AND VACUUM AT 775 K

J. Daniel Whittenberger
National Aeronautics and Space Administration
Lewis Research Center
Cleveland, Ohio 44135-3191

and

E.J. Vesely, Jr.
Surface Engineering Center
IIT Research Institute
30 West 35 Street
Chicago, Illinois 60616-3799

E-5142

ABSTRACT

The solid to liquid phase transformation of LiOH at 744.3 K is considered to be an ideal candidate thermal energy storage (TES) mechanism for a Rankine heat engine based Solar Dynamic system operating at ~682 K. While pure nickel is thought to be a suitable containment material for LiOH, long term containment is of concern because molten hydroxides are usually corrosive. Two commercially pure nickel alloys, Ni-200 and Ni-201, have been exposed to molten LiOH, its vapor and vacuum at 775 K for periods ranging from 50 to 5000 h, and simple mechanical property measurements (77 to 900 K tensile and 750 K creep rupture) of exposed alloys have been undertaken. This report documents the mechanical property test procedures and presents tabular lists of the test data.

INTRODUCTION

In order to provide increased electrical power and thermal energy for Space Station Freedom, NASA is considering solar dynamic systems. The envisioned units will consist of four major components: (1) a focused mirror, (2) a heat receiver, (3) a thermal energy storage system, and (4) a heat engine. The parabolic mirrors will gather sunlight and focus it into receivers which absorb the energy. Part of this energy will be distributed directly to a heat engine driving an electrical generator, and the rest of the energy will be shunted to a thermal energy storage system for use when Space Station Freedom is in Earth's eclipse. From a materials view point the thermal energy storage system is of particular concern, as the solid to liquid transformation of salts is generally the most efficient method to store heat. Hence, the containment materials must be able to withstand long exposures (~30 yr) to molten, highly corrosive salts.

In the case of an organic Rankine Cycle heat engine utilizing toluene as the working fluid, the solid to liquid phase transformation of LiOH has been suggested (ref. 1) as a nearly ideal means for thermal energy storage. This choice is based on (1) a 744.3 K melting temperature, which is close to the maximum operating temperature range (671 to 700 K) for this type of engine;

(2) the high energy storage capacity of 0.87 kJ/g; (3) the low volume change of LiOH (~1 percent) upon solidification (ref. 2); and (4) probable compatibility with pure nickel (ref. 3).

A program has been undertaken to examine the question of long term compatibility between high purity Ni alloys and LiOH. Of prime concern was the possibility that exposure to LiOH would corrode these alloys and lead to failure of the thermal energy storage unit through degradation of the mechanical properties. Nickel specimens have been exposed to molten LiOH, its vapor and vacuum at the Lewis Research Center and subsequently subjected to tensile and creep rupture testing at the Surface Engineering Center of the IIT Research Institute. This report documents the mechanical property test procedures and presents tabular lists of all the generated mechanical property test data. Analysis of the mechanical property data as well as observations concerning the effect(s) of LiOH and vacuum on pure Ni have been presented elsewhere (refs. 4 to 6).

EXPERIMENTAL PROCEDURES

Exposures

Simultaneous exposure of pure Ni alloy samples to liquid LiOH and hydroxide vapor were undertaken at the Lewis Research Center in thin-wall, nominally 280 x 120 x 130 mm "Bread Pan" corrosion capsules. Two racks, each holding about 50 tensile type specimens, resided within the bread pan where, above the melting point of LiOH, the lower rack was covered with molten hydroxide while the second rack was exposed to the LiOH vapor. A third rack of specimens was laid on top of the sealed capsule, and the whole assembly placed inside a vacuum furnace for heat treatment. This latter batch of specimens served as the control to separate the effects of thermal exposure alone from the combined influence of heat and chemical attack experienced by the specimens within the capsule.

Capsules and test specimens were fabricated from the approximately 1.6-mm-thick Ni-200 and Ni-201 alloy sheet, where for any specific experiment the corrosion capsule and test specimens were cut from the same material. Bread Pan capsules with matching lids were produced by a combination of bending and welding, while the clevis tensile type test specimens (fig. 1) were directly punched from the as-received sheet stock. In most cases the gage length of the test specimens was parallel to the sheet rolling direction. Prior to assembly both the tensile specimens and Bread Pans were cleaned by hot vapor degreasing and ultrasonic washing in trichloroethane. After filling capsules with racks of specimens and LiOH granules, they were evacuated and sealed by welding.

Bread Pans were heat treated for various lengths of time at 775 K in vacuum. None of the exposures was continuous; all experienced shutdowns due to various furnace operation problems. Upon completion of the corrosion experiment, the capsules were cut open, and the LiOH dissolved in running water. The LiOH and vacuum exposed specimens were then forwarded to the Surface Engineering Center of the IIT Research Institute for mechanical property testing under contract NAS3-24976.

The chemistry and other data regarding the alloys and LiOH are given in table I. Based on material specifications (ref. 7) for pure nickel alloys, Ni-201 is a low-carbon version Ni-200. However, as can be seen in table I, the present heat of Ni-200 contains lesser amounts of substitutional impurities (Fe, Mn, and Si) as well as a lower C content than the lot of Ni-201.

Tensile Testing

Multiple tensile tests at 77, 298, 400, 600, 750, and 900 K were conducted on LiOH exposed, vacuum annealed, and as-received specimens. Briefly, testing was undertaken in universal screw driven machines at a nominal strain rate of 6.7×10^{-5} s^{-1} through the 0.2 percent yield; beyond this strain the deformation rate was increased to 2.1×10^{-3} mm/s and held until failure. Strain was measured via a mechanical extensometer directly attached to the gage section. The testing atmosphere varied with temperature where (1) at 77 K, specimens were immersed in liquid N_2; (2) at 298 and 400 K, tests were conducted in air; and (3) above 400 K, measurements were carried out in a 0.006 Pa or better vacuum. Typical test data included 0.02 and 0.2 percent offset yield strengths, ultimate tensile strength (UTS) and elongation at failure, where all mechanical properties were calculated on the basis of the original (pre-exposure) dimensions. Tensile testing was undertaken on as-received Ni-200 (table I) and specimens exposed for 401 and 2500 h to molten hydroxide, its vapor or vacuum at 775 K. Additionally Ni-201 (table I) specimens were tested after 0, 50, 400, 2200, and 5000 h exposure to LiOH and vacuum at 775 K.

The incoming specimens (fig. 1) were punched with nominal 25.4 mm gage marks. The exact distance between these points was measured and recorded. Each specimen was then tested according to the procedures outlined below:

<u>77 K Tests</u>

1. Install sample in cold cell grips.
2. Tape load pins in place.
3. Set extensometer bottom grip on sample.
4. Set top extensometer grip on top of sample 25.4 mm from other grip.
5. Install thermocouple tip on sample and hook leads to upper pull rod.
6. Screw assembly into cylinder.
7. Install system into Instron.
8. Pour thermos of liquid N_2 into cold cell slowly (caution: system will sputter and some liquid will be ejected).
9. As the liquid N_2 cools the system, a load will develop on the load cell; readjust crosshead to keep load at zero.
10. After at least 4 flasks are put in, allow system to settle for 8 min while carefully observing load cell. Refill N_2 as needed; N_2 level should be 12 to 25 mm below top of can. This places sample in center of a 305 mm deep volume of liquid nitrogen.
11. Set up Instron and X-Y plotter parameters:
    Instron crosshead speed = 0.127 mm/min (lever in low).
    Instron chart speed = 12.7 mm/min.
    Instron load cell setting = 2273 kg.
    X axis 0.004 V/mm.
    Y axis 0.004 V/mm.
    Pen down.
    Servo to on.
12. Begin test.

13. When load reaches ~450 kg:
    Pen lift.
    Y-axis to 0.02 V/mm.
    Pen record.
14. When extension reaches 1.20 V from starting point:
    Pen lift.
    X-axis to 0.02 V/mm.
    Pen record.
15. When extension reaches 1.25 V from starting point:
    Shift crosshead rate to 0.002 mm/min.
16. When extension reaches 6.5 V:
    Pen lift.
    X-axis to 0.04 V/mm.
    Pen record.
17. Record on data sheet ultimate load from digital display.
18. After sample breaks, turn system off.
19. Remove cold cell from Instron.
20. Dump remaining liquid N_2.
21. Allow unit to warm to room temperature, and remove upper load arm assembly.
22. Remove sample from fixture.
23. Measure sample final width, thickness, and gage length.

Room-Temperature Tests

1-4. Same as 77 K testing.
5. Set up Instron and X-Y plotter parameters:
    Instron crosshead speed = 0.127 mm/min (lever in low).
    Instron chart speed = 12.7 mm/min.
    Instron load cell setting = 2273 kg.
    X axis 0.004 V/mm.
    Y axis 0.004 V/mm.
    Pen down.
    Servo to on.
6. Begin test.
7. When load reaches ~450 kg:
    Pen lift.
    Y-axis to 0.02 V/mm.
    Pen record.
8. When extension reaches 1.20 V from starting point:
    Pen lift.
    X-axis to 0.02 V/mm.
    Pen record.
9. When extension reaches 1.25 V from starting point:
    Shift crosshead rate to 0.002 mm/min.
10. When extension reaches 6.5 V:
    Pen lift.
    X-axis to 0.04 V/mm.
    Pen record.
11. Record on data sheet ultimate load from digital display.
12. After sample breaks, turn system off.
13. Remove sample from fixture.
14. Measure sample final width, thickness, and gage length.

400 K Tests

1-5. Same as 77 K testing.
5. Install system into Instron.
6. Put furnace on unit, and hook up furnace controller.
7. Set controller to 400 K.
8. Alloy system to come to equilibrium at 400 K (estimate 1 h).
9. Set up Instron and X-Y plotter parameters:
   Instron crosshead speed = 0.127 mm/min (lever in low).
   Instron chart speed = 12.7 mm/min.
   Instron load cell setting = 2273 kg.
   X axis 0.004 V/mm.
   Y axis 0.004 V/mm.
   Pen down.
   Servo to on.
10. Begin test.
11. When load reaches ~450 kg:
    Pen lift.
    Y-axis to 0.02 V/mm.
    Pen record.
12. When extension reaches 1.20 V from starting point:
    Pen lift.
    X-axis to 0.02 V/mm.
    Pen record.
13. When extension reaches 1.25 V from starting point:
    Shift crosshead rate to 0.002 mm/min.
14. When extension reaches 6.5 V:
    Pen lift.
    X-axis to 0.04 V/mm.
    Pen record.
15. Record on data sheet ultimate load from digital display.
16. After sample breaks, turn system off.
17. Disconnect furnace controller and remove furnace.
18. Allow unit to cool to room temperature, and remove upper load arm from Instron.
19. Remove sample.
20. Measure sample final width, thickness, and gage length.

600 - 900 K Tests

The three highest temperature tests were run in vacuum. This was accomplished in an IITRI designed a vacuum test chamber. One such vessel is illustrated in figure 2 which shows the general location of the specimen and the high temperature extensometer. The upper load arm exits the chamber by way of a dual O-ring seal area that is connected to a secondary mechanical pump. The main chamber is attached, using standard vacuum components, to a high-vacuum turbomolecular pump. Through use of this technique the main chamber vacuum of 0.006 Pa was repeatedly achieved. Lead-throughs in the hot chamber base plate allowed connections of the following items:

- High-vacuum turbomolecular pump.
- Standard mechanical roughing pump.
- Internal vacuum gage.
- Coax electronic lead-throughs for the extensometer.

- Internal specimen thermocouple.
- Purge port.

Testing at 600 to 900 K followed these steps:

1. Install sample in grips.
2. Set extensometer bottom grip on sample.
3. Set top extensometer grip on top of sample 1 in. from other grip.
4. Install unit on vacuum chamber bottom plate.
5. Install T/C tip on sample and hook leads to lower pull rod.
6. Set up and connect extensometer in chamber.
7. Check and replace O-rings if necessary.
8. Put top on vacuum chamber.
9. Install system into Instron.
10. Place furnace and controller around vacuum chamber.
11. Rough pump vacuum chamber to ~2.6 Pa.
12. Pump vacuum chamber with turbopump.
13. When vacuum in chamber is <0.006 Pa, begin heating.
14. Allow system to come to equilibrium at test temperature.
15. Set up Instron and X-Y plotter parameters:
    Instron crosshead speed = 0.127 mm/min (lever in low).
    Instron chart speed = 12.7 mm/min.
    Instron load cell setting = 2273 kg.
    X axis 0.004 V/mm.
    Y axis 0.004 V/mm.
    Pen down.
    Servo to on.
16. Begin test.
17. When load reaches ~450 kg:
    Pen lift.
    Y-axis to 0.02 V/mm.
    Pen record.
18. When extension reaches 1.20 V from starting point:
    Pen lift.
    X-axis to 0.02 V/mm.
    Pen record.
19. When extension reaches 1.25 V from starting point:
    Shift crosshead rate to 0.002 mm/min.
20. When extension reaches 6.5 V:
    Pen lift.
    X-axis to 0.04 V/mm.
    Pen record.
21. Record on data sheet the ultimate load from digital display.
22. After sample breaks, turn system off.
23. Allow unit to cool to room temperature in a vacuum.
24. Remove unit from Instron.
25. Open vacuum chamber.
26. Remove extensometer and top load arm.
27. Remove sample from bottom load arm.
28. Measure final width, thickness, and gage length of sample.

Creep Rupture Testing

Four standard creep stands with IITRI designed vacuum test vessels, similar to that shown in figure 2, were connected to a high vacuum cryogenic pump. A typical series of creep rupture experiments consisted of 8 samples tested at engineering stress levels designed to produce failure in 50 to 1500 h at 750 K in a vacuum of 6×10^{-3} Pa or better. Appropriate extension - time results were gathered by a data logger tied to each stand with the desired information to include time to 0.1, 0.2, 0.5, 1, 2, 5, and 10 percent strain; steady state creep rate; and failure time & elongation. Ni-200 was tested in the following material conditions: (1) as-received; (2) exposed to molten LiOH for 401 and 2500 h; and (3) annealed in vacuum for 401 and 2500 h. As-received Ni-201 was also tested as well as specimens which had been exposed to molten hydroxide or vacuum for 2200 h and 5000 h.

Prior to testing, the creep rupture specimens were punched with nominal 25.4 mm gage marks, and the exact distance between the gage marks was measured and recorded. Vacuum creep rupture testing at 750 K was undertaken following the procedures outlined below:

1. Install sample in grips.
2. Set extensometer bottom grip on sample.
3. Set top extensometer grip on top of sample 25.4 mm from other grip.
4. Install unit on vacuum chamber bottom plate.
5. Install thermocouple tip on sample and hook leads to lower pull rod.
6. Set up and connect extensometer in chamber.
7. Check and replace O-rings if necessary.
8. Put top on vacuum chamber.
9. Install system into creep stand.
10. Connect vacuum chamber to system.
11. Rough pump vacuum chamber to ~2.6 Pa.
12. Pump vacuum chamber with cryogenic pump.
13. When chamber is <0.006 Pa, begin heating chamber.
14. Allow system to come to equilibrium at 750 K.
15. Using the desired stress level and knowing the cross sectional area of the specimen, calculate the desired dead weight loading required.
16. With the data logger set to scan every 15 s, load the specimen at the desired level.
17. Turn on timer to unit.
18. Continue recording the data every 15 s for 5 minutes; at that time, change scan rate to every 5 minutes.
19. Continue recording every 5 minutes until test time equals 1 h, then change scan time to every hour, for the next 24 h. At that point set scanner to 6 h intervals.
20. When sample breaks, system will turn itself off.
21. Allow unit to cool to room temperature under vacuum.
22. Remove chamber from creep stand and take out specimen.
23. Measure gage section on specimen and transfer that information along with data from datalogger into computer program.
24. Using data, find the following information:
    A. elastic strain
    B. time to 0.1, 0.2, 0.5, 1.0, 2.0, 5.0, and 10.0% strain
    C. time to failure
    D. steady state creep rate.
25. Plot creep curve from data.

RESULTS

The tensile test data, consisting of the 0.02 and 0.2 percent offset yield stress, ultimate tensile strength and tensile elongation, for as-received and exposed Ni-200 and Ni-201 are presented in tables II and III, respectively. Additionally for each test temperature - material condition the following statistical parameters are given: (1) arithmetic average; (2) standard deviation; (3) maximum value; and (4) minimum value. Analysis of these data and typical microstructures of as-received, exposed and tensile tested materials are presented in references 4 to 6.

Tables IV and V summarize the results of creep rupture testing where data for time to 0.1, 0.2, 0.5, 1, 2, 5, and 10 percent strain; steady state (SS) creep rate; and failure time & elongation are presented. Additionally for Ni-200 the creep rates at 2 and 5 percent plastic strain are given; since steady state was not generally reached until 10 percent or more strain had been accumulated. Analysis of the creep rupture behavior along with typical creep curves and plots of the time-to-rupture data and creep rates are presented in reference 6 in addition to photomicrographs of the microstructure of tested samples.

DISCUSSION

An extensive study (refs. 4 to 6) of prolonged exposures of commercially pure Ni alloys to LiOH and vacuum at 775 K has shown that there is little difference in properties after unstressed exposure to either environment for as long as 5000 h. Specifically:

1. No significant weight changes (<1 mg/cm^2) occurred after exposures in either molten LiOH, hydroxide vapor or vacuum;

2. Little, if any, difference in 77 to 900 K tensile properties among vacuum, LiOH vapor or liquid exposed samples could be detected; and

3. 750 K vacuum creep rupture properties of vacuum and molten LiOH exposed specimens are identical.

While surface connected cracks were found in the post-tensile test microstructures of LiOH exposed Ni-200 but not seen in vacuum annealed tensile tested Ni-200, such differences did not translate into measurable changes in mechanical properties. Furthermore, no microstructural differences were observed in Ni-201 exposed to any of the three environments.

No degradation of mechanical properties due to LiOH exposure at 775 K was found in either Ni-200 or Ni-201. However, several major differences between these two alloys were noted: (1) the elevated temperature ductility of the heat of Ni-200 was much better than that of Ni-201, and (2) Ni-200 was free of intergranular cracking, whereas significant intergranular cracking occurred in Ni-201 tested at and above 750 K. This behavior is probably due to the higher purity of the present lot of Ni-200 in comparison to that of Ni-201 (table I).

Although the data indicate that Ni and LiOH are compatible, two potential problems (ref. 5) which have strong implications with respect to a LiOH/Ni thermal energy storage system have been identified:

1. Internal pressurization of the hydroxide filled Ni vessels must be avoided to prevent possible failure of fusion weld joints from a combination of tensile stress and intergranular corrosion, and

2. The slow, but steady, loss of the LiOH energy storage media must be expected if hydrogen can freely permeate through the Ni containment vessel.

Even with these two precautions in mind, it can be concluded that pure Ni is a suitable containment material for a LiOH thermal energy storage system.

SUMMARY

Considerable mechanical property testing of two pure Ni alloys exposed to molten LiOH, its vapor, and vacuum for prolonged periods at 775 K have been undertaken. A complete description of the test procedures and tabular lists of the mechanical property test results are presented in this report.

ACKNOWLEDGMENT

The authors would like to acknowledge S. Cohen, S. Johnson and T. Kerslake of the Solar Dynamic Power and Propulsion Office at the NASA Lewis Research Center for the financial support of this work.

REFERENCES

1. Downing, R.S.; and Parekh, M.B.: Thermal Energy Storage for an Organic Rankine Cycle Solar Dynamic Powered Space Station. Energy for the Twenty-First Century (20th IECEC), Vol. 2, SAE, Warrendale, PA, 1985, pp. 2.397-2.409.

2. Heidenreich, G.R.; and Parekh, M.B.: Thermal Energy Storage for Organic Rankine Cycle Solar Dynamic Space Power Systems. Advancing Toward Technology Breakout in Energy Conversion (21st IECEC), Vol. 2, American Chemical Society, Washington, D.C., 1986, pp. 791-797.

3. DeVries, G.; and Grantham, L.F.: Corrosion of Metals in the Molten LiOH-LiF-H_2O System. Electrochem. Technol., vol. 5, no. 7-8, July-Aug. 1967, pp. 335-340.

4. Whittenberger, J.D.: A Preliminary Report on the Effects of Long-Term Exposure of LiOH on Pure Nickel. J. Mater. Energy Systems, vol. 8, no. 4, Mar. 1987, pp. 385-390.

5. Whittenberger, J.D.: Use of Pure Nickel and LiOH for Thermal Energy Storage. J. Mater. Eng., vol. 10, no. 4, 1988, pp. 247-258.

6. Whittenberger, J.D.: Properties of Pure Nickel Alloys After Long Term Exposures to LiOH and Vacuum at 775 K. Accepted J. Mater. Eng., 1990.

7. Alloy Digest Data Sheets Ni-75 and Ni-139. Engineering Alloys Digest, Inc., Upper Montclair, NJ.

ORIGINAL PAGE IS OF POOR QUALITY

Table I. Characterization of Starting Materials.

Material	Form	Supplier	Heat/Lot Number	Composition (Wt Pct)
Ni 200	Annealed Sheet	Huntington Alloys	K51K2A	0.01C-<0.01Fe-0.22Mn-0.02P-0.001S-0.04Si-bal Ni
Ni 201	Annealed	DVN America	6510	0.02C-0.01Cu-0.06Fe-0.001S-0.16Si-bal Ni
LiOH	Granules	Foote Chemical	503-11B	99.1LiOH-0.3H_2O with Li_2CO_3 + Li_2SO_4 < 1.94, CaO < 0.2, Heavy Metals < 0.002, Trace Cl

Table II(a). Tensile Properties of Ni-200 after Exposure to LiOH at 775 K

	Temp, K	0.02 YS, MPa	0.2 YS, MPa	UTS, MPA	Elong, %	
		As Received Condition				
	77	147.0	252.0	606.0	56.0	
	77	243.0	311.0	603.0	54.0	
	77	-	283.0	608.0	53.0	
Average		195.0	282.0	605.7	54.3	
Std Dev		48.0	24.1	2.1	1.2	
Maximum		243.0	311.0	608.0	56.0	
Minimum		147.0	252.0	603.0	53.0	
	298	-	-	397.0	43.0	
	298	-	-	393.0	39.0	
	298	241.0	260.0	399.0	39.0	
	298	-	-	394.0	42.0	Transverse
	298	199.0	253.0	396.0	45.0	Transverse
Average		220.0	256.5	395.8	41.6	
Std Dev		21.0	3.5	2.1	2.3	
Maximum		241.0	260.0	399.0	45.0	
Minimum		199.0	253.0	393.0	39.0	
	400	193.0	224.0	362.0	31.0	
	400	229.0	234.0	362.0	33.0	
	400	196.0	230.0	361.0	35.0	
Average		206.0	229.3	361.7	33.0	
Std Dev		16.3	4.1	0.5	1.6	
Maximum		229.0	234.0	362.0	35.0	
Minimum		193.0	224.0	361.0	31.0	
	600	172.0	201.0	328.0	38.0	
	600	164.0	211.0	315.0	33.0	
	600	164.0	201.0	325.0	36.0	
Average		166.7	204.3	322.7	35.7	
Std Dev		3.8	4.7	5.6	2.1	
Maximum		172.0	211.0	328.0	38.0	
Minimum		164.0	201.0	315.0	33.0	
	750	95.0	114.0	253.0	48.0	
	750	125.0	155.0	250.0	56.0	
	750	139.0	164.0	274.0	43.0	
	750	133.0	158.0	236.0	52.0	Transverse
	750	-	-	232.0	55.0	Transverse
Average		123.0	147.8	249.0	50.8	
Std Dev		16.9	19.8	13.6	4.8	
Maximum		139.0	164.0	274.0	56.0	
Minimum		95.0	114.0	236.0	43.0	
	900	70.0	79.0	139.0	53.0	
	900	-	-	135.0	42.0	
	900	68.0	76.0	149.0	41.0	
Average		69.0	77.5	141.0	45.3	
Std Dev		1.0	1.5	5.9	5.4	
Maximum		70.0	79.0	149.0	53.0	
Minimum		68.0	76.0	135.0	41.0	

Table II(b). Tensile Properties of Ni-200 after Exposure to LiOH at 775 K

	Temp, K	0.02 YS, MPa	0.2 YS, MPa	UTS, MPA	Elong, %	0.02 YS, MPa	0.2 YS, MPa	UTS, MPA	Elong, %	0.02 YS, MPa	0.2 YS, MPa	UTS, MPA	Elong, %	
		401 h at Temperature												
		Liquid				Vapor				Vacuum				
	77	109.0	132.0	576.0	57.0	-	-	577.0	63.0	124.0	139.0	581.0	61.0	
	77	126.0	137.0	576.0	62.0	82.0	89.0	577.0	59.0	97.0	133.0	579.0	59.0	
	77	-	-	577.0	62.0	112.0	132.0	576.0	61.0	-	-	579.0	63.0	
Average		117.5	134.5	576.3	60.3	97.0	110.5	576.7	61.0	110.5	136.0	579.7	61.0	
Std Dev		8.5	2.5	0.5	2.4	15.0	21.5	0.5	1.6	13.5	3.0	0.9	1.6	
Maximum		126.0	137.0	577.0	62.0	112.0	132.0	577.0	63.0	124.0	139.0	581.0	63.0	
Minimum		109.0	132.0	576.0	57.0	82.0	89.0	576.0	59.0	97.0	133.0	579.0	59.0	
	298	94.0	113.0	367.0	54.0	98.0	117.0	367.0	49.0	112.0	130.0	374.0	54.0	
	298	91.0	111.0	366.0	50.0	86.0	115.0	368.0	53.0	117.0	129.0	372.0	48.0	
	298	94.0	115.0	364.0	56.0	90.0	112.0	366.0	50.0	94.0	118.0	372.0	51.0	
	298	98.0	117.0	362.0	52.0	99.0	114.0	368.0	56.0	92.0	113.0	370.0	51.0	Transverse
	298	96.0	117.0	366.0	51.0	94.0	112.0	367.0	51.0	97.0	106.0	370.0	52.0	Transverse
Average		94.6	114.6	365.0	52.6	93.4	114.0	367.2	51.8	102.4	119.2	371.6	51.2	
Std Dev		2.3	2.3	1.8	2.2	4.9	1.9	0.7	2.5	10.1	9.2	1.5	1.9	
Maximum		98.0	117.0	367.0	56.0	99.0	117.0	368.0	56.0	117.0	130.0	374.0	54.0	
Minimum		91.0	111.0	362.0	50.0	86.0	112.0	366.0	49.0	92.0	106.0	370.0	48.0	
	400	96.0	111.0	336.0	44.0	98.0	114.0	336.0	46.0	105.0	121.0	341.0	43.0	
	400	98.0	113.0	335.0	44.0	91.0	109.0	338.0	44.0	97.0	111.0	340.0	44.0	
	400	96.0	110.0	336.0	46.0	92.0	111.0	337.0	45.0	94.0	112.0	342.0	43.0	
Average		96.7	111.3	335.7	44.7	93.7	111.3	337.0	45.0	98.7	114.7	341.0	43.3	
Std Dev		0.9	1.2	0.5	0.9	3.1	2.1	0.8	0.8	4.6	4.5	0.8	0.5	
Maximum		98.0	113.0	336.0	46.0	98.0	114.0	338.0	46.0	105.0	121.0	342.0	44.0	
Minimum		96.0	110.0	335.0	44.0	91.0	109.0	336.0	44.0	94.0	111.0	340.0	43.0	
	600	91.0	104.0	296.0	42.0	95.0	111.0	298.0	40.0	-	-	308.0	39.0	
	600	88.0	109.0	303.0	38.0	90.0	110.0	297.0	37.0	-	-	308.0	31.0	
	600	86.0	110.0	299.0	38.0	-	-	301.0	38.0	98.0	114.0	305.0	35.0	
Average		88.3	107.7	299.3	39.3	92.5	110.5	298.7	38.3	98.0	114.0	307.0	35.0	
Std Dev		2.1	2.6	2.9	1.9	2.5	0.5	1.7	1.2	0.0	0.0	1.4	3.3	
Maximum		91.0	110.0	303.0	42.0	95.0	111.0	301.0	40.0	98.0	114.0	308.0	39.0	
Minimum		86.0	104.0	296.0	38.0	90.0	110.0	297.0	37.0	98.0	114.0	305.0	31.0	
	750	-	-	223.0	46.0	75.0	95.0	224.0	32.0	82.0	101.0	232.0	48.0	
	750	71.0	94.0	226.0	52.0	73.0	96.0	226.0	52.0	94.0	108.0	235.0	52.0	
	750	81.0	97.0	226.0	48.0	83.0	97.0	227.0	48.0	-	-	201.0	57.0	
	750	82.0	97.0	226.0	53.0	82.0	94.0	228.0	52.0	86.0	107.0	229.0	30.0	Transverse
	750	-	-	225.0	44.0	78.0	94.0	223.0	53.0	-	-	232.0	40.0	Transverse
Average		78.0	96.0	225.2	48.6	78.2	95.2	225.6	47.4	87.3	105.3	225.8	45.4	
Std Dev		5.0	1.4	1.2	3.4	3.9	1.2	1.9	7.9	5.0	3.1	12.5	9.5	
Maximum		82.0	97.0	226.0	53.0	83.0	97.0	228.0	53.0	94.0	108.0	235.0	57.0	
Minimum		71.0	94.0	223.0	44.0	73.0	94.0	223.0	32.0	82.0	101.0	201.0	30.0	
	900	-	-	150.0	66.0	64.0	76.0	143.0	66.0	72.0	86.0	148.0	40.0	
	900	66.0	80.0	146.0	64.0	72.0	81.0	145.0	48.0	-	-	153.0	70.0	
	900	51.0	75.0	145.0	70.0	58.0	77.0	144.0	63.0	61.0	76.0	150.0	67.0	
Average		58.5	77.5	147.0	66.7	64.7	78.0	144.0	59.0	66.5	81.0	150.3	59.0	
Std Dev		7.5	2.5	2.2	2.5	5.7	2.2	0.8	7.9	5.5	5.0	2.1	13.5	
Maximum		66.0	80.0	150.0	70.0	72.0	81.0	145.0	66.0	72.0	86.0	153.0	70.0	
Minimum		51.0	75.0	145.0	64.0	58.0	76.0	143.0	48.0	61.0	76.0	148.0	40.0	

Table II(c). Tensile Properties of Ni-200 after Exposure to LiOH at 775 K

	Temp, K	0.02 YS, MPa	0.2 YS, MPa	UTS, MPA	Elong, %	0.02 YS, MPa	0.2 YS, MPa	UTS, MPA	Elong, %	0.02 YS, MPa	0.2 YS, MPa	UTS, MPA	Elong, %	
						2500 h at Temperature								
		Liquid				Vapor				Vacuum				
	77	103.0	118.0	553.0	62.0	-	-	568.0	48.0	114.0	131.0	584.0	61.0	
	77	107.0	123.0	560.0	57.0	107.0	126.0	564.0	58.0	114.0	129.0	584.0	62.0	
	77	103.0	122.0	559.0	59.0	96.0	123.0	570.0	60.0	110.0	128.0	582.0	64.0	
Average		104.3	121.0	557.3	59.3	101.5	124.5	567.3	55.3	112.7	129.3	583.3	62.3	
Std Dev		1.9	2.2	3.1	2.1	5.5	1.5	2.5	5.2	1.9	1.2	0.9	1.2	
Maximum		107.0	123.0	560.0	62.0	107.0	126.0	570.0	60.0	114.0	131.0	584.0	64.0	
Minimum		103.0	118.0	553.0	57.0	96.0	123.0	564.0	48.0	110.0	128.0	582.0	61.0	
	298	90.0	107.0	359.0	56.0	111.0	121.0	354.0	55.0	100.0	111.0	369.0	53.0	
	298	88.0	108.0	358.0	52.0	85.0	102.0	356.0	54.0	100.0	112.0	369.0	56.0	
	298	71.0	103.0	362.0	50.0	95.0	105.0	356.0	56.0	94.0	114.0	377.0	57.0	
	298	78.0	108.0	354.0	52.0	89.0	101.0	355.0	50.0	104.0	118.0	373.0	57.0	Transverse
	298	105.0	116.0	359.0	48.0	88.0	102.0	358.0	51.0	76.0	89.0	372.0	51.0	Transverse
Average		86.4	108.4	358.4	51.6	93.6	106.2	355.8	53.2	94.8	108.8	372.0	54.8	
Std Dev		11.6	4.2	2.8	2.7	9.3	7.5	1.3	2.3	9.9	10.2	3.0	2.4	
Maximum		105.0	116.0	362.0	56.0	111.0	121.0	358.0	56.0	104.0	118.0	377.0	57.0	
Minimum		71.0	103.0	354.0	48.0	85.0	101.0	354.0	50.0	76.0	89.0	369.0	51.0	
	400	96.0	111.0	326.0	43.0	103.0	117.0	331.0	45.0	89.0	111.0	358.0	45.0	
	400	102.0	116.0	330.0	45.0	96.0	110.0	331.0	48.0	98.0	113.0	334.0	46.0	
	400	93.0	114.0	329.0	45.0	116.0	127.0	329.0	45.0	97.0	112.0	345.0	46.0	
Average		97.0	113.7	328.3	44.3	105.0	118.0	330.3	46.0	94.7	112.0	345.7	45.7	
Std Dev		3.7	2.1	1.7	0.9	8.3	7.0	0.9	1.4	4.0	0.8	9.8	0.5	
Maximum		102.0	116.0	330.0	45.0	116.0	127.0	331.0	48.0	98.0	113.0	358.0	46.0	
Minimum		93.0	111.0	326.0	43.0	96.0	110.0	329.0	45.0	89.0	111.0	334.0	45.0	
	600	84.0	105.0	291.0	42.0	86.0	105.0	296.0	43.0	92.0	114.0	319.0	43.0	
	600	77.0	105.0	291.0	41.0	118.0	126.0	298.0	42.0	87.0	104.0	311.0	38.0	
	600	80.0	102.0	288.0	44.0	76.0	108.0	292.0	42.0	91.0	112.0	309.0	38.0	
Average		80.3	104.0	290.0	42.3	93.3	113.0	295.3	42.3	88.8	109.5	313.0	40.3	
Std Dev		2.9	1.4	1.4	1.2	17.9	9.3	2.5	0.5	2.9	3.8	3.7	2.3	
Maximum		84.0	105.0	291.0	44.0	118.0	126.0	298.0	43.0	92.0	114.0	319.0	43.0	
Minimum		77.0	102.0	288.0	41.0	76.0	105.0	292.0	42.0	85.0	104.0	309.0	38.0	
	750	86.0	91.0	222.0	32.0	80.0	90.0	223.0	54.0	89.0	102.0	230.0	64.0	
	750	78.0	94.0	220.0	52.0	67.0	90.0	223.0	57.0	77.0	96.0	232.0	48.0	
	750	71.0	91.0	215.0	54.0	71.0	88.0	218.0	56.0	70.0	93.0	232.0	61.0	
	750	65.0	86.0	217.0	54.0	73.0	89.0	222.0	52.0	74.0	91.0	231.0	58.0	Transverse
	750	70.0	88.0	216.0	55.0	68.0	86.0	218.0	51.0					Transverse
Average		74.0	90.0	218.0	49.4	71.8	88.6	220.8	54.0	77.5	95.5	231.3	57.8	
Std Dev		7.3	2.8	2.6	8.8	4.6	1.5	2.3	2.3	7.1	4.2	0.8	6.0	
Maximum		86.0	94.0	222.0	55.0	80.0	90.0	223.0	57.0	89.0	102.0	232.0	64.0	
Minimum		65.0	86.0	215.0	32.0	67.0	86.0	218.0	51.0	70.0	91.0	230.0	48.0	
	900	53.0	69.0	146.0	62.0	55.0	72.0	146.0	38.0	61.0	78.0	159.0	39.0	
	900	-	-	141.0	61.0	50.0	70.0	148.0	53.0	61.0	74.0	154.0	45.0	
	900	60.0	72.0	144.0	53.0	54.0	69.0	148.0	59.0					
Average		56.5	70.5	143.7	58.7	53.0	70.3	147.3	50.0	60.7	76.7	155.3	50.0	
Std Dev		3.5	1.5	2.1	4.0	2.2	1.2	0.9	8.8	0.5	1.9	2.6	11.6	
Maximum		60.0	72.0	146.0	62.0	55.0	72.0	148.0	59.0	61.0	78.0	159.0	66.0	
Minimum		53.0	69.0	141.0	53.0	50.0	69.0	146.0	38.0	60.0	74.0	153.0	39.0	

Table III(a). Tensile Properties of Ni-201 after Exposure to LiOH at 775 K

	Temp, K	0.02 YS, MPa	0.2 YS, MPa	UTS, MPA	Elong, %
			As Received Condition		
	77	183.0	240.0	657.0	57.0
	77	190.0	241.0	653.0	60.0
	77	186.0	230.0	648.0	63.0
Average		186.3	237.0	652.7	60.0
Std Dev		2.9	5.0	3.7	2.4
Maximum		190.0	241.0	657.0	63.0
Minimum		183.0	230.0	648.0	57.0
	298	139.0	198.0	434.0	45.0
	298	152.0	201.0	440.0	44.0
	298	162.0	211.0	436.0	44.0
Average		151.0	203.3	436.7	44.3
Std Dev		9.4	5.6	2.5	0.5
Maximum		162.0	211.0	440.0	45.0
Minimum		139.0	198.0	434.0	44.0
	400	131.0	186.0	410.0	41.0
	400	164.0	201.0	416.0	38.0
	400	174.0	201.0	411.0	42.0
Average		156.3	196.0	412.3	40.3
Std Dev		18.4	7.1	2.6	1.7
Maximum		174.0	201.0	416.0	42.0
Minimum		131.0	186.0	410.0	38.0
	600	146.0	173.0	384.0	25.0
	600	147.0	184.0	400.0	37.0
	600	149.0	179.0	399.0	33.0
Average		147.3	178.7	394.3	31.7
Std Dev		1.2	4.5	7.3	5.0
Maximum		149.0	184.0	400.0	37.0
Minimum		146.0	173.0	384.0	25.0
	750	119.0	144.0	250.0	13.0
	750	121.0	145.0	259.0	13.0
	750	-	-	227.0	10.0
Average		120.0	144.5	245.3	12.0
Std Dev		1.0	0.5	13.5	1.4
Maximum		121.0	145.0	259.0	13.0
Minimum		119.0	144.0	227.0	10.0
	900	79.0	100.0	160.0	11.0
	900	81.0	98.0	168.0	14.0
	900	74.0	100.0	159.0	10.0
Average		78.0	99.3	162.3	11.7
Std Dev		2.9	0.9	4.0	1.7
Maximum		81.0	100.0	168.0	14.0
Minimum		74.0	98.0	159.0	10.0

Table III(b). Tensile Properties of Ni-201 after Exposure to LiOH at 775 K

50 h at Temperature

	Temp, K	0.02 YS, MPa	0.2 YS, MPa	UTS, MPA	Elong, %	0.02 YS, MPa	0.2 YS, MPa	UTS, MPA	Elong, %	0.02 YS, MPa	0.2 YS, MPa	UTS, MPA	Elong, %	
		Liquid				Vapor				Vacuum				
	77	98.0	173.0	641.0	60.0	169.0	187.0	637.0	64.0	171.0	182.0	646.0	62.0	
	77	160.0	187.0	643.0	62.0	155.0	179.0	642.0	63.0	183.0	192.0	645.0	60.0	
	77	162.0	178.0	642.0	61.0	172.0	183.0	641.0	58.0	175.0	187.0	649.0	58.0	
Average		140.0	179.3	642.0	61.0	165.3	183.0	640.0	61.7	176.3	187.0	646.7	60.0	
Std Dev		29.7	5.8	0.8	0.8	7.4	3.3	2.2	2.6	5.0	4.1	1.7	1.6	
Maximum		162.0	187.0	643.0	62.0	172.0	187.0	642.0	64.0	183.0	192.0	649.0	62.0	
Minimum		98.0	173.0	641.0	60.0	155.0	179.0	637.0	58.0	171.0	182.0	645.0	58.0	
	298	158.0	195.0	433.0	47.0	146.0	155.0	455.0	49.0	158.0	171.0	432.0	49.0	
	298	154.0	170.0	432.0	50.0	136.0	145.0	426.0	48.0	150.0	189.0	430.0	48.0	
	298	144.0	150.0	430.0	46.0	136.0	142.0	433.0	50.0	138.0	149.0	430.0	49.0	
	298	135.0	154.0	431.0	51.0	141.0	153.0	423.0	51.0	133.0	150.0	431.0	52.0	Transverse
Average		147.8	167.3	431.5	48.5	139.8	148.8	434.3	49.5	144.8	164.8	430.8	49.5	
Std Dev		9.0	17.7	1.1	2.1	4.1	5.4	12.5	1.1	9.8	16.5	0.8	1.5	
Maximum		158.0	195.0	433.0	51.0	146.0	155.0	455.0	51.0	158.0	189.0	432.0	52.0	
Minimum		135.0	150.0	430.0	46.0	136.0	142.0	423.0	48.0	133.0	149.0	430.0	48.0	
	400	-	-	410.0	41.0	-	-	414.0	41.0	-	-	414.0	41.0	
	400	-	-	407.0	43.0	145.0	160.0	414.0	43.0	137.0	150.0	415.0	43.0	
	400	141.0	151.0	411.0	41.0	-	-	413.0	43.0	131.0	146.0	409.0	44.0	
Average		141.0	151.0	409.3	41.7	145.0	160.0	413.7	42.3	134.0	148.0	412.7	42.7	
Std Dev		0.0	0.0	1.7	0.9	0.0	0.0	0.5	0.9	3.0	2.0	2.6	1.2	
Maximum		141.0	151.0	411.0	43.0	145.0	160.0	414.0	43.0	137.0	150.0	415.0	44.0	
Minimum		141.0	151.0	407.0	41.0	145.0	160.0	413.0	41.0	131.0	146.0	409.0	41.0	
	600	107.0	138.0	389.0	40.0	112.0	140.0	398.0	43.0	117.0	148.0	397.0	41.0	
	600	119.0	147.0	430.0	38.0	117.0	151.0	412.0	44.0	111.0	135.0	390.0	42.0	
	600	101.0	136.0	392.0	42.0	118.0	140.0	392.0	41.0	113.0	143.0	404.0	42.0	
Average		109.0	140.3	403.7	40.0	115.7	143.7	400.7	42.7	113.7	142.0	397.0	41.7	
Std Dev		7.5	4.8	18.7	1.6	2.6	5.2	8.4	1.2	2.5	5.4	5.7	0.5	
Maximum		119.0	147.0	430.0	42.0	118.0	151.0	412.0	44.0	117.0	148.0	404.0	42.0	
Minimum		101.0	136.0	389.0	38.0	112.0	140.0	392.0	41.0	111.0	135.0	390.0	41.0	
	750	101.0	120.0	270.0	39.0	92.0	117.0	268.0	35.0	106.0	129.0	263.0	38.0	
	750	103.0	122.0	287.0	47.0	88.0	112.0	266.0	43.0	-	-	275.0	46.0	
	750	99.0	122.0	279.0	38.0	108.0	123.0	272.0	41.0	107.0	126.0	276.0	47.0	
	750	100.0	120.0	266.0	40.0	98.0	117.0	267.0	38.0	97.0	118.0	270.0	46.0	Transverse
Average		100.8	121.0	275.5	41.0	96.5	117.3	268.3	39.3	103.3	124.3	271.0	44.3	
Std Dev		1.5	1.0	8.1	3.5	7.5	3.9	2.3	3.0	4.5	4.6	5.1	3.6	
Maximum		103.0	122.0	287.0	47.0	108.0	123.0	272.0	43.0	107.0	129.0	276.0	47.0	
Minimum		99.0	120.0	266.0	38.0	88.0	112.0	266.0	35.0	97.0	118.0	263.0	38.0	
	900	68.0	89.0	169.0	14.0	73.0	92.0	158.0	8.0	87.0	104.0	182.0	19.0	
	900	81.0	96.0	160.0	14.0	87.0	103.0	174.0	14.0	82.0	93.0	165.0	14.0	
	900	86.0	101.0	169.0	11.0	74.0	97.0	166.0	11.0	85.0	104.0	181.0	11.0	
Average		78.3	95.3	166.0	13.0	78.0	97.3	166.0	11.0	84.7	100.3	176.0	14.7	
Std Dev		7.6	4.9	4.2	1.4	6.4	4.5	6.5	2.4	2.1	5.2	7.8	3.3	
Maximum		86.0	101.0	169.0	14.0	87.0	103.0	174.0	14.0	87.0	104.0	182.0	19.0	
Minimum		68.0	89.0	160.0	11.0	73.0	92.0	158.0	8.0	82.0	93.0	165.0	11.0	

Table III(c). Tensile Properties of Ni-201 after Exposure to LiOH at 775 K

	Temp, K	0.02 YS, MPa	0.2 YS, MPa	UTS, MPA	Elong, %	0.02 YS, MPa	0.2 YS, MPa	UTS, MPA	Elong, %	0.02 YS, MPa	0.2 YS, MPa	UTS, MPA	Elong, %	
							400 h at Temperature							
		Liquid				Vapor				Vacuum				
	77	145.0	171.0	638.0	61.0	143.0	169.0	637.0	63.0	138.0	166.0	635.0	60.0	
	77	158.0	170.0	639.0	62.0	146.0	181.0	639.0	63.0	160.0	168.0	631.0	61.0	
	77	162.0	191.0	635.0	64.0	142.0	154.0	631.0	68.0	146.0	169.0	631.0	61.0	
Average		155.0	177.3	637.3	62.3	143.7	168.0	635.7	64.7	148.0	167.7	632.3	60.7	
Std Dev		7.3	9.7	1.7	1.2	1.7	11.0	3.4	2.4	9.1	1.2	1.9	0.5	
Maximum		162.0	191.0	639.0	64.0	146.0	181.0	639.0	68.0	160.0	169.0	635.0	61.0	
Minimum		145.0	170.0	635.0	61.0	142.0	154.0	631.0	63.0	138.0	166.0	631.0	60.0	
	298	123.0	132.0	422.0	50.0	125.0	133.0	418.0	51.0	122.0	133.0	420.0	51.0	
	298	117.0	132.0	423.0	51.0	122.0	131.0	420.0	52.0	115.0	131.0	420.0	51.0	
	298	137.0	153.0	417.0	51.0	151.0	190.0	423.0	49.0	119.0	133.0	428.0	51.0	
	298	115.0	135.0	424.0	51.0	123.0	144.0	418.0	50.0	121.0	137.0	418.0	52.0	Transverse
Average		123.0	138.0	421.5	50.8	130.3	149.5	419.8	50.5	119.3	133.5	421.5	51.3	
Std Dev		8.6	8.7	2.7	0.4	12.0	23.9	2.0	1.1	2.7	2.2	3.8	0.4	
Maximum		137.0	153.0	424.0	51.0	151.0	190.0	423.0	52.0	122.0	137.0	428.0	52.0	
Minimum		115.0	132.0	417.0	50.0	122.0	131.0	418.0	49.0	115.0	131.0	418.0	51.0	
	400	105.0	124.0	392.0	44.0	110.0	122.0	399.0	45.0	119.0	134.0	403.0	46.0	
	400	104.0	131.0	410.0	45.0	167.0	183.0	406.0	43.0	121.0	140.0	400.0	45.0	
	400	103.0	140.0	403.0	45.0	80.0	129.0	400.0	44.0	109.0	128.0	403.0	44.0	
Average		104.0	131.7	401.7	44.7	119.0	144.7	401.7	44.0	116.3	134.0	402.0	45.0	
Std Dev		0.8	6.5	7.4	0.5	36.1	27.3	3.1	0.8	5.2	4.9	1.4	0.8	
Maximum		105.0	140.0	410.0	45.0	167.0	183.0	406.0	45.0	121.0	140.0	403.0	46.0	
Minimum		103.0	124.0	392.0	44.0	80.0	122.0	399.0	43.0	109.0	128.0	400.0	44.0	
	600	108.0	129.0	385.0	39.0	108.0	130.0	382.0	38.0	101.0	125.0	379.0	42.0	
	600	109.0	130.0	379.0	35.0	106.0	128.0	377.0	38.0	105.0	125.0	370.0	36.0	
	600	130.0	155.0	371.0	37.0	96.0	123.0	379.0	40.0	108.0	130.0	374.0	34.0	
Average		115.7	138.0	378.3	37.0	103.3	127.0	379.3	38.7	104.7	126.7	374.3	37.3	
Std Dev		10.1	12.0	5.7	1.6	5.2	2.9	2.1	0.9	2.9	2.4	3.7	3.4	
Maximum		130.0	155.0	385.0	39.0	108.0	130.0	382.0	40.0	108.0	130.0	379.0	42.0	
Minimum		108.0	129.0	371.0	35.0	96.0	123.0	377.0	38.0	101.0	125.0	370.0	34.0	
	750	94.0	111.0	256.0	22.0	68.0	101.0	262.0	44.0	77.0	102.0	260.0	45.0	
	750	91.0	110.0	260.0	21.0	84.0	104.0	261.0	47.0	91.0	112.0	277.0	41.0	
	750	86.0	102.0	250.0	23.0	82.0	117.0	269.0	41.0	72.0	102.0	266.0	49.0	
	750	92.0	112.0	262.0	29.0	98.0	114.0	270.0	44.0	86.0	110.0	271.0	43.0	Transverse
Average		90.8	108.8	257.0	23.8	83.0	109.0	265.5	44.0	81.5	106.5	268.5	44.5	
Std Dev		2.9	4.0	4.6	3.1	10.6	6.7	4.0	2.1	7.4	4.6	6.3	3.0	
Maximum		94.0	112.0	262.0	29.0	98.0	117.0	270.0	47.0	91.0	112.0	277.0	49.0	
Minimum		86.0	102.0	250.0	21.0	68.0	101.0	261.0	41.0	72.0	102.0	260.0	41.0	
	900	62.0	86.0	157.0	18.0	74.0	87.0	167.0	20.0	72.0	88.0	161.0	19.0	
	900	70.0	86.0	163.0	20.0	70.0	116.0	161.0	17.0	71.0	88.0	158.0	19.0	
	900	72.0	84.0	156.0	18.0	72.0	89.0	164.0	21.0	69.0	83.0	155.0	15.0	
Average		68.0	85.3	158.7	18.7	72.0	97.3	164.0	19.3	70.7	86.3	158.0	17.7	
Std Dev		4.3	0.9	3.1	0.9	1.6	13.2	2.4	1.7	1.2	2.4	2.4	1.9	
Maximum		72.0	86.0	163.0	20.0	74.0	116.0	167.0	21.0	72.0	88.0	161.0	19.0	
Minimum		62.0	84.0	156.0	18.0	70.0	87.0	161.0	17.0	69.0	83.0	155.0	15.0	

Table III(d). Tensile Properties of Ni-201 after Exposure to LiOH at 776 K

	Temp, K	0.02 YS, MPa	0.2 YS, MPa	UTS, MPA	Elong, %	0.02 YS, MPa	0.2 YS, MPa	UTS, MPA	Elong, %	0.02 YS, MPa	0.2 YS, MPa	UTS, MPA	Elong, %	
								2200 h at Temperature						
		Liquid				Vapor				Vacuum				
	77	-	-	632.0	53.0	148.0	159.0	628.0	64.0	168.0	201.0	626.0	61.0	
	77	163.0	170.0	629.0	66.0	138.0	160.0	628.0	61.0	146.0	169.0	635.0	60.0	
	77	159.0	165.0	642.0	68.0	155.0	168.0	630.0	65.0	-	-	618.0	65.0	
Average		161.0	167.5	634.3	62.3	147.0	162.3	628.7	63.3	157.0	185.0	626.3	62.0	
Std Dev		2.0	2.5	5.6	6.6	7.0	4.0	0.9	1.7	11.0	16.0	6.9	2.2	
Maximum		163.0	170.0	642.0	68.0	155.0	168.0	630.0	65.0	168.0	201.0	635.0	65.0	
Minimum		159.0	165.0	629.0	53.0	138.0	159.0	628.0	61.0	146.0	169.0	618.0	60.0	
	298	118.0	128.0	418.0	53.0	109.0	118.0	417.0	52.0	103.0	118.0	417.0	52.0	
	298	123.0	133.0	414.0	57.0	177.0	185.0	414.0	52.0	95.0	110.0	409.0	52.0	
	298	108.0	123.0	411.0	54.0	152.0	163.0	416.0	52.0	138.0	148.0	414.0	52.0	
	298	109.0	120.0	419.0	52.0	126.0	134.0	409.0	52.0	100.0	112.0	415.0	53.0	Transverse
Average		114.5	126.0	415.5	54.0	141.0	150.0	414.0	52.0	109.0	122.0	413.8	52.3	
Std Dev		6.3	4.9	3.2	1.9	25.8	25.9	3.1	0.0	17.0	15.3	2.9	0.4	
Maximum		123.0	133.0	419.0	57.0	177.0	185.0	417.0	52.0	138.0	148.0	417.0	53.0	
Minimum		108.0	120.0	411.0	52.0	109.0	118.0	409.0	52.0	95.0	110.0	409.0	52.0	
	400	94.0	98.0	384.0	46.0	112.0	121.0	388.0	45.0	87.0	105.0	331.0	45.0	
	400	-	-	392.0	47.0	92.0	104.0	344.0	45.0	101.0	112.0	342.0	43.0	
	400	137.0	170.0	398.0	47.0	85.0	100.0	339.0	45.0	-	-	388.0	45.0	
Average		115.5	134.0	391.3	46.7	96.3	108.3	357.0	45.0	94.0	108.5	353.7	44.3	
Std Dev		21.5	36.0	5.7	0.5	11.4	9.1	22.0	0.0	7.0	3.5	24.7	0.9	
Maximum		137.0	170.0	398.0	47.0	112.0	121.0	388.0	45.0	101.0	112.0	388.0	45.0	
Minimum		94.0	98.0	384.0	46.0	85.0	100.0	339.0	45.0	87.0	105.0	331.0	43.0	
	600	87.0	105.0	349.0	27.0	94.0	109.0	368.0	34.0	101.0	110.0	364.0	38.0	
	600	-	-	362.0	38.0	-	-	367.0	40.0	-	-	367.0	39.0	
	600	97.0	113.0	367.0	33.0	-	-	367.0	37.0	88.0	109.0	356.0	34.0	
Average		92.0	109.0	359.3	32.7	94.0	109.0	367.3	37.0	94.5	109.5	362.3	37.0	
Std Dev		5.0	4.0	7.6	4.5	0.0	0.0	0.5	2.4	6.5	0.5	4.6	2.2	
Maximum		97.0	113.0	367.0	38.0	94.0	109.0	368.0	40.0	101.0	110.0	367.0	39.0	
Minimum		87.0	105.0	349.0	27.0	94.0	109.0	367.0	34.0	88.0	109.0	356.0	34.0	
	750	84.0	100.0	256.0	26.0	71.0	87.0	226.0	38.0	59.0	74.0	231.0	46.0	
	750	80.0	95.0	244.0	19.0	65.0	82.0	226.0	41.0	74.0	96.0	230.0	31.0	
	750	75.0	104.0	324.0	43.0	-	-	225.0	46.0	-	-	219.0	31.0	
	750	63.0	83.0	226.0	32.0	65.0	80.0	225.0	31.0	62.0	77.0	223.0	37.0	Transverse
Average		75.5	95.5	262.5	30.0	67.0	83.0	225.5	39.0	65.0	82.3	225.8	36.3	
Std Dev		7.9	7.9	37.1	8.8	2.8	2.9	0.5	5.4	6.5	9.7	5.0	6.1	
Maximum		84.0	104.0	324.0	43.0	71.0	87.0	226.0	46.0	74.0	96.0	231.0	46.0	
Minimum		63.0	83.0	226.0	19.0	65.0	80.0	225.0	31.0	59.0	74.0	219.0	31.0	
	900	58.0	74.0	144.0	15.0	60.0	73.0	143.0	15.0	60.0	72.0	138.0	13.0	
	900	-	-	141.0	15.0	61.0	74.0	144.0	15.0	59.0	72.0	136.0	13.0	
	900	76.0	81.0	144.0	21.0	78.0	87.0	142.0	16.0	65.0	75.0	141.0	16.0	
Average		67.0	77.5	143.0	17.0	66.3	78.0	143.0	15.3	61.3	73.0	138.3	14.0	
Std Dev		9.0	3.5	1.4	2.8	8.3	6.4	0.8	0.5	2.6	1.4	2.1	1.4	
Maximum		76.0	81.0	144.0	21.0	78.0	87.0	144.0	16.0	65.0	75.0	141.0	16.0	
Minimum		58.0	74.0	141.0	15.0	60.0	73.0	142.0	15.0	59.0	72.0	136.0	13.0	

Table III(e). Tensile Properties of Ni-201 after Exposure to LiOH at 775 K

	Temp, K	0.02 YS, MPa	0.2 YS, MPa	UTS, MPA	Elong, %	0.02 YS, MPa	0.2 YS, MPa	UTS, MPA	Elong, %	0.02 YS, MPa	0.2 YS, MPa	UTS, MPA	Elong, %	
							5000 h at Temperature							
			Liquid				Vapor				Vacuum			
	77	122.0	158.0	627.0	50.0	145.0	161.0	621.0	49.0	206.0	216.0	621.0	69.0	
	77	134.0	145.0	632.0	45.0	132.0	155.0	632.0	45.0	142.0	158.0	627.0	66.0	
	77	-	-	621.0	64.0	142.0	156.0	631.0	53.0	143.0	155.0	628.0	54.0	
Average		128.0	150.5	626.7	53.0	139.7	157.3	628.0	49.0	163.7	176.3	625.3	63.0	
Std Dev		6.0	5.5	4.5	8.0	5.6	2.8	5.0	3.3	29.9	28.1	3.1	6.5	
Maximum		134.0	156.0	632.0	64.0	145.0	161.0	632.0	53.0	206.0	216.0	628.0	69.0	
Minimum		122.0	145.0	621.0	45.0	132.0	155.0	621.0	45.0	142.0	155.0	621.0	54.0	
	298	121.0	129.0	410.0	54.0	112.0	125.0	411.0	52.0	104.0	125.0	405.0	54.0	
	298	113.0	122.0	414.0	54.0	106.0	119.0	412.0	54.0	101.0	119.0	407.0	24.0	
	298	125.0	134.0	412.0	51.0	111.0	124.0	411.0	56.0	104.0	114.0	405.0	52.0	
	298	105.0	119.0	409.0	54.0	106.0	121.0	411.0	53.0	115.0	125.0	408.0	51.0	Transverse
Average		116.0	126.0	411.3	53.3	108.8	122.3	411.3	53.8	106.0	120.8	406.3	45.3	
Std Dev		7.7	5.9	1.9	1.3	2.8	2.4	0.4	1.5	5.3	4.8	1.3	12.3	
Maximum		125.0	134.0	414.0	54.0	112.0	125.0	412.0	56.0	115.0	125.0	408.0	54.0	
Minimum		105.0	119.0	409.0	51.0	106.0	119.0	411.0	52.0	101.0	114.0	405.0	24.0	
	400	91.0	110.0	376.0	44.0	98.0	113.0	376.0	42.0	156.0	177.0	377.0	42.0	
	400	107.0	121.0	384.0	41.0	95.0	113.0	377.0	43.0	98.0	119.0	375.0	39.0	
	400	106.0	121.0	382.0	45.0	99.0	113.0	375.0	42.0	129.0	148.0	374.0	41.0	
Average		101.3	117.3	380.7	43.3	97.3	113.0	376.0	42.3	127.7	148.0	375.3	40.7	
Std Dev		7.3	5.2	3.4	1.7	1.7	0.0	0.8	0.5	23.7	23.7	1.2	1.2	
Maximum		107.0	121.0	384.0	45.0	99.0	113.0	377.0	43.0	156.0	177.0	377.0	42.0	
Minimum		91.0	110.0	376.0	41.0	95.0	113.0	375.0	42.0	98.0	119.0	374.0	39.0	
	600	93.0	113.0	346.0	31.0	84.0	111.0	341.0	28.0	84.0	110.0	345.0	34.0	
	600	89.0	92.0	342.0	35.0	90.0	107.0	356.0	38.0	85.0	116.0	334.0	25.0	
	600	75.0	97.0	325.0	26.0	90.0	111.0	325.0	27.0	88.0	109.0	320.0	25.0	
Average		85.7	100.7	337.7	30.7	88.0	109.7	340.7	31.0	85.7	111.7	333.0	28.0	
Std Dev		7.7	9.0	9.1	3.7	2.8	1.9	12.7	5.0	1.7	3.1	10.2	4.2	
Maximum		93.0	113.0	346.0	35.0	90.0	111.0	356.0	38.0	88.0	116.0	345.0	34.0	
Minimum		75.0	92.0	325.0	26.0	84.0	107.0	325.0	27.0	84.0	109.0	320.0	25.0	
	750	85.0	99.0	242.0	21.0	85.0	103.0	244.0	16.0	94.0	107.0	239.0	24.0	
	750	82.0	99.0	239.0	20.0	89.0	102.0	238.0	17.0	83.0	99.0	254.0	17.0	
	750	73.0	91.0	242.0	20.0	74.0	98.0	223.0	16.0	141.0	152.0	219.0	14.0	
	750	81.0	98.0	242.0	21.0	77.0	91.0	243.0	22.0	84.0	97.0	232.0	16.0	Transverse
Average		80.3	96.8	241.3	20.5	81.3	98.5	237.0	17.8	100.5	113.8	236.0	17.8	
Std Dev		4.4	3.3	1.3	0.5	6.0	4.7	8.4	2.5	23.8	22.4	12.6	3.8	
Maximum		85.0	99.0	242.0	21.0	89.0	103.0	244.0	22.0	141.0	152.0	254.0	24.0	
Minimum		73.0	91.0	239.0	20.0	74.0	91.0	223.0	16.0	83.0	97.0	219.0	14.0	
	900	69.0	82.0	150.0	12.0	70.0	80.0	156.0	12.0	96.0	100.0	132.0	6.0	
	900	145.0	160.0	161.0	13.0	73.0	84.0	154.0	10.0	67.0	81.0	160.0	15.0	
	900	75.0	85.0	147.0	9.0	67.0	76.0	148.0	8.0	65.0	72.0	148.0	11.0	
Average		96.3	109.0	152.7	11.3	70.0	80.0	152.7	10.0	76.0	84.3	146.7	10.7	
Std Dev		34.5	36.1	6.0	1.7	2.4	3.3	3.4	1.6	14.2	11.7	11.5	3.7	
Maximum		145.0	160.0	161.0	13.0	73.0	84.0	156.0	12.0	96.0	100.0	160.0	15.0	
Minimum		69.0	82.0	147.0	9.0	67.0	76.0	148.0	8.0	65.0	72.0	132.0	6.0	

Table IV. 750 K Vacuum Creep Rupture of LiOH Exposed Ni-200.

Material Condition	Stress, MPa	Time to Percent Creep, h 0.1	0.2	0.5	1.0	2.0	5.0	10.0	Rupture	Elongation at end Test or Rupture, Pct	SS Creep Rate, s-1	Creep Rate at 2 Pct Strain, s-1	Creep Rate at 5 Pct Strain, s-1
As Rec	148				0.34	2.89	20.00	112.00	607	55	6.78E-08	1.05E-06	3.35E-07
As Rec	133				0.41	2.55	25.00	153.00	>1026	31	3.56E-08	8.86E-07	2.48E-07
As Rec	104	8.00	18.00	42.00	92.00	205.00	602.00		>1628	14	7.92E-09	2.75E-08	2.33E-08
As Rec	89	19.00	104.00	341.00	545.00	1042.00			>1628	4	6.89E-09	*7.22E-09	*7.22E-09
As Rec	74	119.00	288.00	520.00					>1482	1	*3.00E-09	*3.30E-09	*3.30E-09
As Rec	59	110.00	357.00	649.00					>1482	0.4	*9.97E-10	-	-
L/401h	193						0.01	0.10	10	62	4.72E-06	2.06E-03	2.06E-03
L/401h	177	0.05	0.08	0.20	0.70	2.70			69	42	3.33E-08	1.06E-06	1.00E-07
L/401h	162			0.01	0.04	0.29	2.00	16.50	102	57	6.11E-07	8.00E-06	2.04E-06
L/401h	155	0.01	0.02	0.07	0.30	1.30	8.00	42.30	159	31	3.06E-07	2.32E-06	7.30E-07
L/401h	148				0.01	0.01	2.60	150.00	459	61	3.89E-07	-	1.10E-06
L/401h	133		0.03	0.20	0.90	4.70	40.30	240.00	1307	60	5.00E-08	6.20E-07	1.24E-07
L/401h	117				0.03	3.00	71.00	250.00	1539	49	7.78E-08	7.20E-07	7.78E-08
L/401h	103		0.03	3.80	109.00	304.00	627.00		>1560	4	1.33E-08	1.35E-08	1.36E-08
V/401h	193						0.01	0.30	22	51	3.89E-06	1.46E-03	1.46E-03
V/401h	177						0.01	2.00	76	68	8.33E-07	1.16E-03	1.51E-04
V/401h	162			0.05	0.19	1.60	15.00	118.00	477	56	3.89E-08	1.31E-06	3.16E-07
V/401h	155		0.02	0.09	0.28	0.80	2.70	12.70	177	67	6.11E-07	5.25E-06	3.38E-06
V/401h	148	0.02	0.09	0.70	2.80	8.50	59.20	333.00	740	45	3.33E-08	3.58E-07	9.05E-08
V/401h	133		0.01	0.25	1.60	6.20	36.20	216.00	819	48	5.28E-08	5.51E-07	1.91E-07
V/401h	117				0.10	8.40	111.00	419.00	>1492	17	1.61E-08	1.71E-07	6.39E-08
V/401h	103	0.07	0.40	6.90	34.60	164.00	1350.00		>1461	6	6.94E-09	8.50E-09	6.94E-09
L/2500h	192			0.02	0.04	0.10	0.70		6	37	-	2.72E-05	5.58E-06
L/2500h	177	0.04	0.12	0.50					97	46			
L/2500h	162		0.03	0.06	0.10	0.50			81	33	1.92E-06	5.88E-06	1.92E-06
L/2500h	155			0.03	0.13	0.50	3.80	22.00	1487	60	5.56E-07	8.31E-06	1.11E-06
L/2500h	148		0.02	0.49	1.00	2.00	12.00		120	38	6.94E-07	1.35E-06	6.94E-07
L/2500h	141					0.20	43.20	425.00	1349	36	2.78E-08	3.33E-06	1.04E-07
L/2500h	133	0.02	0.07	0.18	2.70	41.60	694.00		>1509	26	5.00E-09	4.65E-08	5.23E-09
L/2500h	118					0.10	11.90	93.00	>1528	40	4.44E-08	6.50E-06	3.06E-07
V/2500h	193	0.10	0.60	1.00	1.90				24	22	1.81E-06	-	1.81E-06
V/2500h	177			0.02	0.10	0.30	2.30	15.00	67	38	7.78E-07	1.06E-05	2.21E-06
V/2500h	162		0.02	0.14	1.00	2.00	15.30	96.00	500	49	7.78E-08	4.29E-06	3.36E-07
V/2500h	155		0.03	0.10	0.30	1.30	11.30	71.00	329	53	1.53E-07	2.11E-06	4.57E-07
V/2500h	148	0.02	0.10	0.80	1.10	2.20	21.00		400	31	9.44E-08	1.56E-06	6.20E-07
V/2500h	140								404	54			
V/2500h	133	0.06	0.15	1.20	7.30	38.30	105.00	284.00	>1508	23	1.08E-08	1.46E-07	1.46E-07
V/2500h	117		0.04	0.40	3.20	17.50	174.00		>1967	23	2.22E-08	1.38E-07	2.39E-08

Table V. 750 K Vacuum Creep Rupture of LiOH Exposed Ni-201.

Material Condition	Stress, MPa	Time to Percent Creep, h 0.1	0.2	0.5	1.0	2.0	5.0	10.0	Rupture	Elongation at end Test or Rupture, Pct	SS Creep Rate, s-1
As Rec	87	8.50	90.00	360.00	978.00				>1512	2.6	2.19E-09
As Rec	94	12.00	38.50	85.00	186.00				287.0	3.9	1.17E-08
As Rec	101	40.00	87.00	300.00	517.00				1459.0	6.9	3.89E-09
As Rec	109	80.00	240.00	530.00					>1694	0.5	1.06E-09
As Rec	114	1.00	2.00	24.50	94.00				364.4	-	1.25E-08
As Rec	131		0.03	1.40	10.00				38.4	2.0	8.06E-08
As Rec	138				0.66	9.00			28.7	2.9	2.06E-07
As Rec	145	0.02	0.04	0.05	0.17				0.4	5.7	1.06E-05
L/2200h	87			1.40					>1102	0.5	2.29E-10
L/2200h	87								540.3		
L/2200h	94								>1500		
L/2200h	94	6.00	9.20	70.00	156.00	572.00			>1500	4.0	6.00E-09
L/2200h	101	0.50	3.00	25.40	132.00	384.00			>1696	5.0	5.75E-09
L/2200h	109			4.70	104.00				481.0	8.0	4.17E-09
L/2200h	114		0.04	2.00	20.00	103.00			252.0	4.0	2.00E-08
L/2200h	131	0.05	0.20	2.20	12.00	40.00	154.00		161.0	11.0	3.58E-08
L/2200h	138					1.00	125.00		166.0	13.4	2.44E-08
L/2200h	145				0.04	1.00			142.0	9.0	6.42E-09
V/2200h	87		1.80	65.90	363.00				>1171.3	2.6	2.59E-09
V/2200h	87								250.8		
V/2200h	94	0.93	8.10	92.00	1509.00	1523.00			>1531	2.8	2.08E-10
V/2200h	101	34.60	96.20	281.00	597.00				>1457	2.4	2.94E-09
V/2200h	109								> 680		
V/2200h	109			3.80	35.00				76.0	4.2	1.58E-08
V/2200h	114								>1561.2	0.8	
V/2200h	131				0.02	3.00	121.00		260.0	6.2	4.61E-08
V/2200h	138	0.03	0.20	12.40	56.00	150.00			210.0	9.1	2.14E-08
V/2200h	145					0.08	31.00		94.0	9.2	1.31E-07
L/5000h	87	2.00	19.00	93.00	453.00	1053.00			1200.0	8	4.72E-09
L/5000h	94			0.16	54.00	533.00			>1500	9.0	1.92E-09
L/5000h	101				7.00	188.00			>1200	6.0	3.89E-09
L/5000h	109				8.00	105.00	691.00		>1500	8.0	8.33E-09
L/5000h	114	0.20	0.80	1.50	3.00	6.00	130.00		700.0	9.0	2.78E-08
L/5000h	131		19.00	400.00	700.00				>1000.	3.0	6.39E-09
L/5000h	138					0.40	44.00		120.0	9.0	5.00E-08
L/5000h	145					2.00	67.00		160.0	8.0	5.00E-08
V/5000h	87	200.00	547.00						>1400	2.0	3.61E-10
V/5000h	94		1.40	52.00	917.00				>1500	4.0	1.22E-09
V/5000h	101			5.00	84.00	391.00			>1500	7.0	9.44E-09
V/5000h	109			0.08	10.00	110.00			900.0	7.0	7.22E-09
V/5000h	114			0.25	21.00				50.0	6.0	4.17E-08
V/5000h	131					62.00	500.00		700.0	9.0	1.86E-08
V/5000h	138					0.40			24.0	5.0	1.67E-07
V/5000h	145						6.00		98.0	10.0	3.06E-07

NASA
National Aeronautics and Space Administration

Report Documentation Page

1. Report No. NASA TM-102403	2. Government Accession No.	3. Recipient's Catalog No.
4. Title and Subtitle Mechanical Properties of Pure Nickel Alloys After Long Term Exposure to LiOH and Vacuum at 775 K		5. Report Date January 1990
		6. Performing Organization Code
7. Author(s) J. Daniel Whittenberger and E.J. Vesely, Jr.		8. Performing Organization Report No. E-5142
		10. Work Unit No. 474-46-20
9. Performing Organization Name and Address National Aeronautics and Space Administration Lewis Research Center Cleveland, Ohio 44135-3191		11. Contract or Grant No.
		13. Type of Report and Period Covered Technical Memorandum
12. Sponsoring Agency Name and Address National Aeronautics and Space Administration Washington, D.C. 20546-0001		14. Sponsoring Agency Code

15. Supplementary Notes

J. Daniel Whittenberger, NASA Lewis Research Center; E.J. Veseley, Jr., Surface Engineering Center, IIT Research Institute, 30 West 35 Street, Chicago, Illinois 60616-3799.

16. Abstract

The solid to liquid phase transformation of LiOH at 744.3 K is considered to be an ideal candidate thermal energy storage (TES) mechanism for a Rankine heat engine based Solar Dynamic system operating at ~682 K. While pure nickel is thought to be a suitable containment material for LiOH, long term containment is of concern because molten hydroxides are usually corrosive. Two commercially pure nickel alloys, Ni-200 and Ni-201, have been exposed to molten LiOH, its vapor and vacuum at 775 K for periods ranging from 50 to 5000 h, and simple mechanical property measurements (77 to 900 K tensile and 750 K creep rupture) of exposed alloys have been undertaken. This report documents the mechanical property test procedures and presents tabular lists of the test data.

17. Key Words (Suggested by Author(s)) Pure Ni Thermal energy storage LiOH Rankine heat engine	18. Distribution Statement Unclassified – Unlimited Subject Category 26

19. Security Classif. (of this report) Unclassified	20. Security Classif. (of this page) Unclassified	21. No of pages 22	22. Price* A03

NASA FORM 1626 OCT 86

*For sale by the National Technical Information Service, Springfield, Virginia 22161

ORIGINAL PAGE IS OF POOR QUALITY

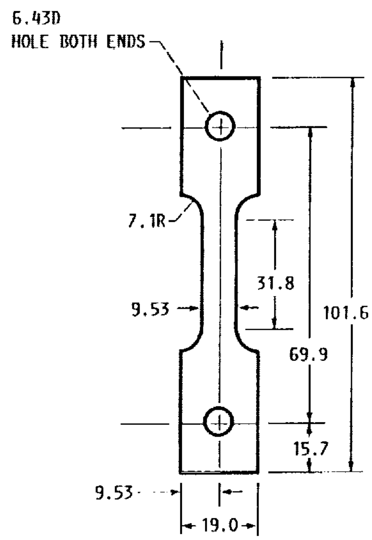

FIGURE 1. - TENSILE SPECIMEN GEOMETRY; ALL DIMENSIONS IN MILLIMETERS.

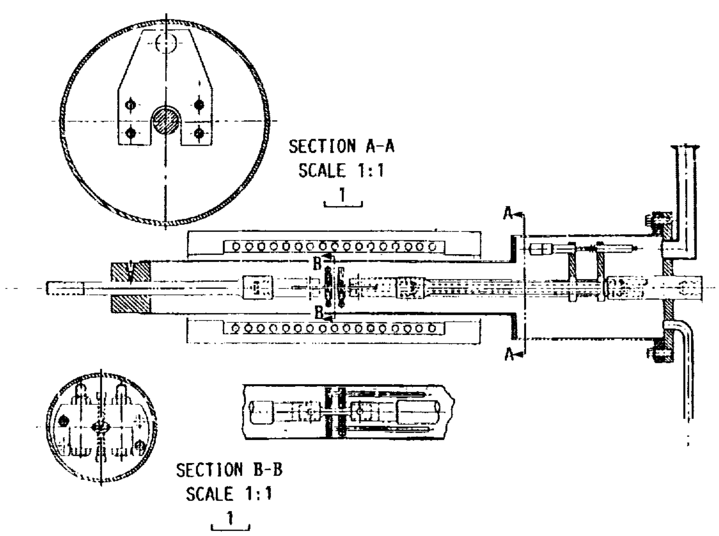

FIGURE 2. - SCHEMATIC DRAWING OF THE HOT VACUUM CHAMBER UTILIZED FOR HIGH TEMPERATURE TENSILE AND CREEP RUPTURE TESTING OF LiOH/VACUUM EXPOSED PURE Ni ALLOYS.